COLLAPSE OF A CYLINDRICAL CAVITY IN A FLUID LAYER UNDER IMPACT

É. I. Andriankin, V. K. Bobolev,
and A. V. Dubovik

The case of impact on a thin annular fluid layer with a gas-filled cavity is considered. The solution of the problem reduces to integrating a system of two first-order ordinary differential equations. The equations are analyzed qualitatively, and some exact solutions are found. Cases are noted of pulsation of the cavity, and the influence of counter-pressure and viscosity is investigated. The experimental results obtained are in agreement with the numerical computations carried out herein.

The problem of the collapse of a cavity in a fluid is one of the fundamental problems of hydrodynamics. It is not only of theoretical but also of practical interest since the collapse of cavities often occurs in the lubrication layer of bearings, during cavitation, during testing the sensitivity of liquid explosives to impact, etc. A number of papers [1-8] are devoted to the analysis of these questions, where the collapse of a spherical cavity has been investigated. In contrast to these, let us examine the case of impact at a velocity w_0 on an annular fluid layer of thickness h_0 with outer radius a and inner radius b. The solution of this problem turns out to be somewhat more complex than in the case of the collapse of a spherical bubble because of the presence of an axial velocity component, a finite radius of the impactor a, and a time-varying layer thickness.

The hydrodynamic equations describing the collapse of a cavity will be written in a cylindrical coordinate system as

$$\frac{\partial v}{\partial z}+\frac{1}{r}\frac{\partial ru}{\partial r}=0, \qquad \frac{\partial p}{\partial z}=0 \tag{1}$$

$$\frac{\partial u}{\partial t}+u\frac{\partial u}{\partial r}+v\frac{\partial u}{\partial z}=-\frac{1}{\rho_0}\frac{\partial p}{\partial r}+\frac{\mu}{\rho_0}\frac{\partial^2 u}{\partial z^2} \tag{2}$$

The layer is considered thin $h_0 \ll a$ so that the pressure depends only on the radius, and the velocity $v \sim hu/a$ along the z axis turns out to be much less than the radial fluid velocity u. Hence, the equation of motion in projections on the z axis is satisfied to second-order accuracy in h/a as in boundary-layer theory.

Let us neglect the compressibilities of the fluid, the impactor, and the anvil. Since the mass of the load m usually turns out to be much greater than the mass of the fluid, then the impactor motion can be considered uniform, $w_0 = \text{const} < 0$, down to quite small thicknesses of the impressed layer. This assumption simplifies the mathematical investigation of the problem since the equation of motion of the load

$$\frac{dw}{dt}=\frac{2\pi}{m}\int_b^a pr\,dr, \qquad h=h_0+\int_0^t w\,dt \tag{3}$$

is satisfied automatically if $m \to \infty$, and $w = w_0$.

Moscow. Translated from Zhurnal Prikladnoi Mekhaniki i Tekhnicheskoi Fiziki, No. 6, pp. 98-106, November-December, 1970. Original article submitted December 1, 1969.

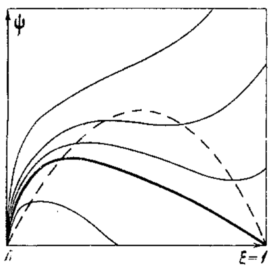

Fig. 1

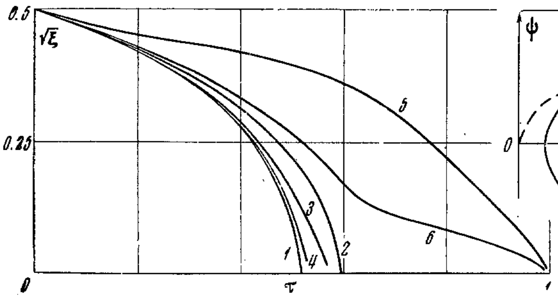

Fig. 2

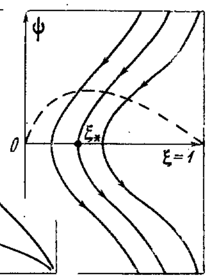

Fig. 3

Compression of the gas in the cavity can be considered adiabatic, and the velocity of sound in the gas is much greater than the velocity of the cavity boundary $r_+^{\cdot}$. Hence, the pressure within the cavity will be identical throughout and equal to

$$p_+ = p_0 (b / r_+)^{2\gamma} (h_0 / h)^{\gamma} \tag{4}$$

Let us first examine the case when the inertial forces predominate over the viscosity forces:

$$\rho u h^2 / \mu a > 1 \tag{5}$$

i.e., let us investigate collapse of a cavity in an ideal fluid.

The flow of an ideal fluid will be irrotational; hence, a particular solution can be found for an arbitrary layer thickness in the case $w_0 = \text{const}$. This is easily established if the equations of motion are written in the Gromeka–Lamb form.

Let us seek the solution for v in the form

$$v = v_0 z, \quad v_0 = w_0 / h, \quad h = h_0 + w_0 t, \quad w_0 < 0 \tag{6}$$

then it follows from the continuity equation and utilization of the boundary condition $u(r_+, t) = r_+^{\cdot}$ that

$$u = -\frac{v_0 r}{2} + \frac{q}{r}, \quad q = r_+ r_+^{\cdot} + \frac{v_0}{2} r_+^2 \tag{7}$$

and the pressure is found from (2) and (4):

$$\frac{p}{\rho_0} = \frac{v_0^{\cdot}}{4}(r^2 - r_+^2) - q^{\cdot} \ln\frac{r}{r_+} + \frac{r_+^{\cdot 2} - u^2}{2} + \frac{p_0}{\rho_0}\left(\frac{b}{r_+}\right)^{2\gamma}\left(\frac{h_0}{h}\right)^{\gamma} \tag{8}$$

The equation for r_+ follows from the condition on the outer radius of the impactor $p(a, t) = p_0$. In the dimensionless quantities

$$\xi = \left(\frac{r_+}{a}\right)^2, \quad z_1 = \frac{h}{a}, \quad \tau = \frac{|w_0| t}{h_0}, \quad \varepsilon = \frac{h_0}{a}, \quad \beta = \left(\frac{b}{a}\right)^2, \quad \lambda = \frac{8 p_0 \varepsilon^2}{\rho_0 w_0^2} \tag{9}$$

this equation is

$$\begin{gathered} 2\xi \ln\xi (1-\tau)\frac{d\psi}{d\tau} = (1-\xi)[(\psi+\xi)^2 - 3\xi] - 2\xi^2 \ln\xi + \lambda(1-\tau)^2 \xi \left\{\left[\frac{\beta}{(1-\tau)\xi}\right]^{\gamma} - 1\right\}, \\ \frac{d\xi}{d\tau} = -\frac{\psi}{1-\tau}, \quad z_1 = \varepsilon(1-\tau) \end{gathered} \tag{10}$$

The velocity and the position of the cavity radius, i.e.,

$$\psi(0) = \psi_0, \quad \xi(0) = \beta$$

will be the initial conditions for (10).

Difficulties in formulating the boundary conditions do not arise in a wave analysis of the impact process. The scheme of impact on an incompressible fluid is suitable only with the time $t_0 \gg a/c_0$, when the sound waves interacting repeatedly will cause motion of the whole layer. Within the scope of the theory of an incompressible fluid it is assumed that $c_0 \to \infty$, so that $t_0 \to 0$, but infinite forces must be introduced,

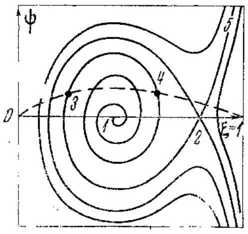

Fig. 4

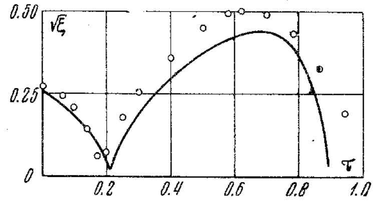

Fig. 5

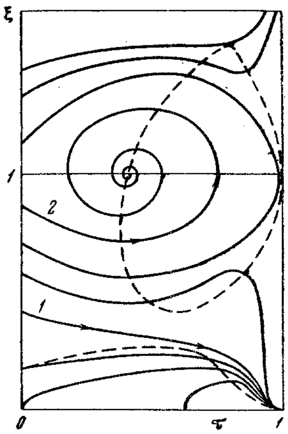

Fig. 6

which will cause a finite flow velocity in an infinitesimal time interval $(0, t_0)$. However, this velocity turns out to be less than in the side unloading waves.

To find the initial velocity of motion and therefore the quantity ψ_0, let us apply the law of conservation of momentum in projections on the radius to half the layer, and let us pass to the limit:

$$\lim_{t_0 \to 0} \int_0^{t_0} dt \int_{r_+}^{a} p\, dr = \rho_0 h \int_{r_+}^{a} ur\, dr$$

Substituting the expression for the velocity and the pressure taken from (7) and (8) into this relationship and taking into account that $r_+(0) = b$, we find

$$\psi_0 = \frac{\beta - \beta \ln \beta - 1}{\ln \beta}, \qquad q(0) = \frac{w_0 a (\beta - 1)}{2 \varepsilon \ln \beta} \tag{11}$$

Using (7), (8), and (11), the initial velocities of the motion on the outer u_- and inner u_+ boundaries of the layer as well as the initial position of the neutral line r° can be determined:

$$u_-(0) = -\frac{w_0 \psi_0}{2\varepsilon} > 0, \quad u_+(0) = \frac{w_0 \psi_0}{2\varepsilon \sqrt{\beta}}, \quad \left(\frac{r^\circ}{a}\right)^2 = \frac{\beta - 1}{\ln \beta} \tag{12}$$

For the maximum pressure,where $(\partial p / \partial r)_{r = r_*} = 0$, we will have

$$\left(\frac{r_*}{a}\right)^2 = \frac{(\beta - 1)[3 \beta \ln^2 \beta - (1 - \beta)^2]}{2 \beta (\ln \beta)^3} \tag{13}$$

Since $\beta < 1$, it then follows from (12) that at the initial instant the discharge within occurs more rapidly than outside $u_+(0) > |u_-(0)|$. It can also be shown from (13) that as $t \to 0$ the neutral line is farther from the center than the position of the maximum pressure, so that there exists a zone within the layer where the flow is opposite to the pressure gradient. Such a situation facilitates the origination of instability.

Let us investigate the behavior of the solution of the system (10) in two cases when the pressures within p_+ and outside p_- the cavity equal zero and when there exists an internal pressure in the cavity but $p_- = 0$, and moreover, $\gamma = 2$. In these cases one first-order equation can be obtained from the system (10):

$$2 \psi \xi \ln \xi \frac{d\psi}{d\xi} = (1 - \xi)[3\xi - (\psi + \xi)^2] + 2 \xi^2 \ln \xi - \frac{\lambda \beta^2}{\xi}, \quad \psi(\beta) = \psi_0(\beta) \tag{14}$$

In the case of no counterpressure ($\lambda = 0$) the field of integral curves of (14) is pictured in Fig. 1. The ψ axis is a singular solution, and the ξ axis is the isocline of the infinities. The isocline of the zeroes for $\lambda = 0$

$$\psi = -\xi \pm \left(3\xi + \frac{2\xi^2 \ln \xi}{1 - \xi} - \frac{\lambda \beta^2}{\xi(1 - \xi)}\right)^{1/2} \tag{15}$$

intersects the ξ axis at two singular points. The point $\xi = 0$, $\psi = 0$ is a node, and the integral curves are tangent to the ψ axis according to the law

$$\psi = A / \sqrt{|\ln \xi|}, \qquad A = \text{const} \tag{16}$$

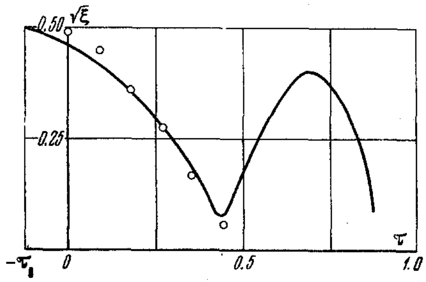

Fig. 7

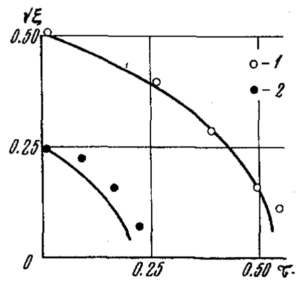

Fig. 8

The point $\xi = 1$, $\psi = 0$ is a saddle point with the slopes of the separatrices $K_{1,2} = 1/2\,(1 \pm \sqrt{3})$ so that $K_2 > (d\psi_0/d\xi)_1$, and hence, the separating curve passes below the isocline of zeroes (dashes in Fig. 1). Considering $\psi\ (\xi)$ a known function, we can find from (10)

$$\ln(1-\tau) = \int\limits_{\beta}^{\xi} \frac{d\xi}{\psi} \tag{17}$$

It is seen from (16) that this integral converges, and therefore, collapse of the cavity occurs within the finite time $\tau_k < 1$.

Numerical integration of (10) for the case $\beta = 0.25$ and $\lambda = 0$ yielded $\tau_k \approx 0.517$ respectively (see curve 1 in Fig. 2). Presented in this same Fig. 2 are the computed curves for $\lambda = 0.313$, curve 3, and $\lambda = 0.078$, curve 4. It is seen from the behavior of the curves that the counterpressure turns out to be substantial at the end since the gas pressure $p \sim (h_0 b^2/h r_+^2)^\gamma$ rapidly rises for small r_+.

At the time of collapse the velocity u_+ grows infinitely; however, the integral of the energy E converges:

$$u_+ \sim \frac{1}{r_+\sqrt{\ln r_+}}, \quad E \sim \lim \int\limits_{r_+}^{a} \rho_0 (u^2 + v^2)\, r\, dr\ (r_+ \to 0)$$

The flow and its associated energy dissipation rebuild after collapse.

Let us now examine another case ($p_- = 0, \gamma = 2$) for which $p_+ > 0$ and the gas in the cavity plays the part of an elastic piston. If $\lambda\beta^2 > K_*$, which is determined from the condition

$$K_* = \max\,[3\xi^2 (1-\xi) + 2\xi^3 \ln \xi]$$

that the radicand in (15) is negative in the range $0 < \xi < 1$, then there are no singularities in the strip $0 \leq \xi \leq 1$; the integral curves intersect the ξ axis with the infinite derivative ($\psi \sim \sqrt{\xi - \xi_*}$) and approach the line $\xi = 1$ (Fig. 3) with the asymptotic

$$\psi^2 = -\lambda\beta^2 \ln (1-\xi) + \text{const} \tag{18}$$

The radius of the cavity diminishes initially (the dashes denote the line of the initial conditions) to the value $\sqrt{\xi_*(\beta)}$ but then again grows (since ψ becomes negative) tending to unity, which physically denotes splashes of the whole fluid. The splashing occurs for a finite layer thickness at the time $\tau_k < 1$ since the integral (17) converges as $\xi \to \xi_*$.

If $\lambda\beta^2 < K_*$, then the behavior of the integral curves is complicated substantially and is indicative of an oscillatory mode. In fact, let $\lambda\beta^2$ be small; then the isocline of zeroes ψ_0 intersects the ξ axis, the isocline of the infinities, at two singularities ξ_1 and ξ_2 respectively located close to $\xi = 0$ and $\xi = 1$. Using this in the series expansion of the right side of (14) in the neighborhood of the singularities, it is easy to establish that the singularity $(\xi_1, 0)$ is a focus and $(\xi_2, 0)$ is a saddle point with slopes $(d\psi_0/d\xi)_2 \approx \pm 1$ of the separatrices. The isocline of zeroes at the point $(0, \xi_2)$ has the slope $(d\psi_0/d\xi)_2 \approx 2/(1-\xi_2)^2$.

The asymptotic of the integral curves for $\xi \to 1$ is given by (18).

Near the focus, (14) reduces to

$$\frac{d\psi}{d\Delta} = \frac{3\Delta + \xi_1\psi}{\psi\xi_1 \ln \xi_1}, \qquad \xi = \xi_1 + \Delta$$

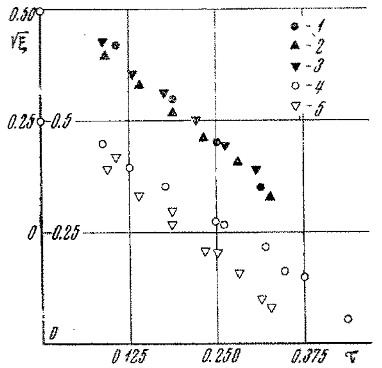

Fig. 9

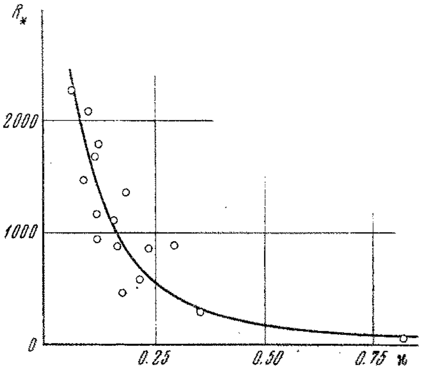

Fig. 10

It follows from its solution

$$r^2 \sim \frac{A\xi_1 |\ln \xi_1|}{\cos^2 \varphi} \exp K\xi_1\varphi, \qquad A > 0, \qquad K > 0$$

that the integral curves issue from the focus as is pictured in Fig. 4. It is seen from Fig. 4 that one or more oscillations of the cavity occur before the splashing depending on whether the initial condition belongs to any curve of the focus (section 3–4 on the line of initial conditions, dashed in Fig. 4) or not.

Splashing occurs during $\tau_k < 1$ for all solutions excepting the separatrix 5–2. Approaching the ψ axis along it, the integral (17) diverges ($\psi \sim \xi - \xi_2$), and $\tau_k \to 1$. It is hence interesting that the radius of the gas cavity tends to the limit at a finite time of compression. The pressure in the problem without a cavity [6, 9] rises infinitely as $h \to 0$ according to the law

$$p \sim \frac{3}{4} \frac{\rho_0 a^2 w_0^2}{h^2} \left[1 - \left(\frac{r}{a}\right)^2\right]$$

but for $\gamma = 2$ and $r_+ \to r_k$ the pressure in the gas cavity also rises proportionately to

$$p_0 (b^2 h_0 / r_k^2 h)^\gamma \sim 1 / h^2$$

hence, this case is also possible.

In the cases $\gamma \neq 2$, where the system (10) does not reduce to one equation, the behavior of the solution can be assessed from a comparison with the particular cases (14) already examined.

For example, it is evident that if β is close to one, then splashing will occur under impact since a finite rise in pressure during compression in a finite time can extrude a sufficiently thin layer of fluid.

It has been found by a numerical computation for the case $\beta = 0.9$, $\varepsilon = 0.1$, and $\gamma = 1.4$, for example, that $\tau \approx 0.4$ at the time of the splash.

If oscillations of the cavity occurred and its radius turned out to be sufficiently small, then for $\gamma < 2$ it can diminish to zero since for finite r_k the pressure in the fluid, which rises according to the law $\sim h^{-2}$, would become greater than the pressure in the gas $\sim h^{-\gamma}$. This case is analogous to the problem without counterpressure $\lambda = 0$. Hence, collapse occurs for a finite layer thickness. Majorizing the asymptotic for ψ as $\tau \to \tau_k$ in the form

$$\psi^2 = A \int_{\xi_0}^{\xi} \frac{d\xi}{\xi^\gamma \ln \xi} > A \int_{\xi_0}^{\xi} \frac{d\xi}{\xi \ln \xi} = A \ln \left| \ln \frac{\xi}{\xi_0} \right|, \quad A = \lambda \beta^\gamma (1 - \tau_k)^{2-\gamma}$$

it is easy to establish that the integral (17) converges, and therefore $\tau_k < 1$. These modes are observed even in a numerical computation (the solid line in Fig. 5). For $\gamma > 2$ and sufficiently small r_k a rapid rise in pressure in the cavity results in splashing.

A computation for the case $\gamma = 3$, $\beta = 0.25$, $\varepsilon = 0.05$ showed that up to the time $\tau \approx 0.23$ the cavity has almost collapsed but then starts to expand and splashing occurs at $\tau \approx 0.5$.

Now, let us consider viscous fluid flow when the inertial forces are small and the ratio (5) becomes less than unity. It follows from the equation of motion that

$$u = f(r, t)\,\eta(1-\eta)$$
$$\eta = z / h, \quad h = h_0 + w_0 t \tag{19}$$

Using the continuity equation and the boundary condition v (h, t) $= w_0$, we find

$$f = -\frac{3 w_0 r}{h} + \frac{6q}{r}, \quad v = w_0 \eta^2 (3 - 2\eta) \tag{20}$$

Let us satisfy the condition on the cavity boundary $r = r_+(t)$ in the mean:

$$r_+^{\cdot} = \int_0^1 u(r_+, t)\, d\eta \tag{21}$$

thereby averting a cumulative splash at $\eta = 1/2$, to which the parabolic velocity profile reduces. It follows from (10) and (21) that

$$q = r_+ r_+^{\cdot} + {}^1/_2\, w_0 r_+^2 / h \tag{22}$$

Substituting (19), (20), and (22) into the equation of motion, we find

$$p = \frac{2\mu}{h^2}\left[\frac{3 w_0 (r^2 - r_+^2)}{2h} - 6q \ln\frac{r}{r_+}\right] + p_0 \left(\frac{b^2 h_0}{r_+^2 h}\right)^{\gamma} \tag{23}$$

Using the boundary condition p $(a$, t) $= p_0$ and transforming to dimensionless quantities, we obtain an equation for the cavity radius:

$$(1-\tau)\ln\xi \frac{d\xi}{d\tau} = 1 + \xi\ln\xi - \xi + \delta(1-\tau)^3\left\{1 - \left[\frac{\beta}{\xi(1-\tau)}\right]^{\gamma}\right\}$$
$$\xi(0) = \beta, \quad \delta = \frac{a p_0}{3\mu|w_0|}\left(\frac{h_0}{a}\right)^3 \tag{24}$$

This equation is easily integrated in the absence of counterpressure:

$$\tau = 1 - \frac{1 + \beta\ln\beta - \beta}{1 + \xi\ln\xi - \xi}$$

The graph of this function is pictured in Fig. 2 (curve 2). It is also easy to find the solution under the condition of no fluid flowing to the outside from (22), i.e., when u $(a$, t) $=0$:

$$\tau = 1 - \frac{1-\beta}{1-\xi}$$

To a certain extent this solution characterizes the blocking role of the viscosity.

An increase in viscosity diminishes the fluid discharge at a constant pressure gradient. However, let us note that under impact on a viscous layer the pressure rises [6, 9] as μ increases so that the mass balance is conserved.

The field of integral curves of (24) is pictured in Fig. 6. The $\tau = 1$ axis is a singular solution, and the $\xi = 0$ and $\xi = 1$ axes are isoclines of the infinities. The isoclines of zeroes (dashed in Fig. 6) intersect the isoclines of infinities at three singularities. Let us note that it is convenient to assume, say, $\gamma = 1.5$ for the image of the isocline of zeroes; then a quadratic equation is obtained in $1-\tau$. The singularity $\tau = 1$, $\xi = 1$ is a saddle point near which the solution is

$$(1-\xi)^2 = \frac{(1-\tau)^{4/3}}{10} + \frac{\text{const}}{1-\tau}$$

At the singularity $\tau = 1$, $\xi = 0$, a node, the integral curves merge with the asymptotic

$$\xi = (1-\tau)^n / \beta\delta^{1/\gamma}, \quad n = (3-\gamma)/\gamma$$

which has a zero tangent for $\gamma < 2$. The kind of singularity $\tau = 1-\beta$, $\xi = 1$ is determined by the law $\Delta = 1 - 4/\gamma\delta\beta^2$. If $\Delta < 0$, then the singularity is a focus. The case $\Delta > 0$ (a saddle-point singularity) is less probable since δ is usually small and $\beta < 1$.

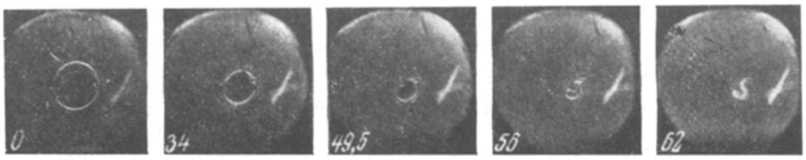

Fig. 11

Expanding the coefficients of (24) in series near $\xi = 1 + y$, $\tau = 1 - \beta + x$, we find

$$dy / dx = \gamma\beta^2\delta - \gamma\beta\delta x / y$$

Integrating this equation, we easily establish that the focus is twisted. Thus, for example, for small δ we obtain

$$r^2 \approx \frac{A}{\sin^2\varphi} \exp\left(-\gamma\beta^2\delta \operatorname{arc\,tg} \frac{\operatorname{tg}\varphi}{\gamma\beta\delta}\right), \; A > 0$$

At the beginning of the motion the cavity is always diminished since $(d\xi/d\tau)_+ < 0$. It is seen from the behavior of the integral curves that complete collapse occurs when the solution (curve 1) enters the node. For large cavity radii when β is close to unity, the solution can belong to a focus (curve 2), and therefore, splashing will occur for $\tau < 1$. For the case $\beta = 0.9$, $\delta = 0.695$ a computation showed that the splashing already occurs at $\tau = 0.142$. This does not contradict the physics of the phenomenon since as $b \to a$ and for finite h the viscous drag $\sim \mu w_0 a (a-b)/h^3$ turns out to be less than the counterpressure $\sim h^{1-\gamma} b^{1-2\gamma}$. Collapse occurs because of the rapid growth $\sim h^{-3}$ of the maximum pressure in the fluid.

As computations showed and as has been observed in tests, the influence of counterpressure on the velocity of collapse in the viscous mode (in contrast to the inertial) is quite substantial (curves 5, 6, and 2 in Fig. 2, calculated for $\delta = 0.695$, $\delta = 0.0865$, and $\delta = 0$). This is easily understood since the viscous drag diminishes the velocity of collapse, and hence, for cavity radii r_+ equal to the inertial solution, the thickness of the viscous layer turns out to be less.

The case when the inertial and viscous forces are of the same order is sometimes interesting. Let us assume that the velocity profile is hence parabolic. It is hence possible to utilize (19) and (20) to evaluate the derivatives $\partial u/\partial t$, $\partial^2 u/\partial r^2$, $\partial p/\partial r$, and $\partial^2 u/\partial z^2$ in (2). Then averaging the equation of motion with respect to z, we obtain

$$\begin{gathered} 2\xi \ln \xi (1-\tau)\frac{d\psi}{d\tau} = 1.2(1-\xi)[(\xi+\psi)^2-\xi] + 2\xi\psi\ln\xi \\ + \lambda\xi(1-\tau)^2\left\{\left[\frac{\beta}{\xi(1-\tau)}\right]^\gamma - 1\right\} - \frac{\nu\xi}{1-\tau_*}[1-\xi+(\psi+\xi)\ln\xi] \\ \nu = \frac{24}{R}, \quad R = \frac{\rho_0 h_0 |w_0|}{\mu} \end{gathered} \tag{25}$$

In the limit when inertial forces can be neglected, this equation automatically goes over into (24). However, the motion of an ideal fluid is obtained only approximately as $\nu \to 0$. This is also conceivable since the velocity profile was considered independent of the Reynolds number R from the very beginning. In fact, the boundary layer grows gradually. Hence, the solution of (10) at the time when the boundary layers on the impactor and the anvil are joined [9] can be taken as the initial condition for (25).

Now, let us describe some experimental results. The method of conducting the experiment has been expounded in detail in [10]. The radius of the air cavity compressed by the impact of a load in a fluid layer of given thickness was measured by a photographic method. The investigated fluids were nitroglycerine $\rho_0 = 1.6$ g/cm^3 and $\mu = 0.3$ poise and a solution of glycerine in water $\rho_0 = 1.24$ g/cm^3 and $\mu = 3$ poise. The impact velocity of a 5-kgf load varied between 1 and 4 m/sec. The thicknesses of the fluid layers were 0.25 – 1.0 mm, and the radius of the impactor was 10 mm. The altitudes of the 5- and 10-mm-diameter air cavities corresponded to the thicknesses of the fluid layers.

Values of the experimental results averaged over several tests in parallel are superimposed by circles in Fig. 5 in the coordinates $\sqrt{\xi}$, τ for the case $\beta = 1/16$, $\varepsilon = 0.05$, $\lambda = 0.313$, and $\delta = 0.695$. A comparison with a theoretical computation (solid line) shows good agreement even during oscillation (pulsation) of the cavity.

Experiment is also compared with a computation for the case $\beta = 0.25$, $\varepsilon = 0.05$, $\lambda = 0.313$, $\delta = 0.695$ in Fig. 7. The theory can be in good agreement with experiment if the initial instant is chosen from the condition that the velocities in the computation and the experiment are equal at $\tau_0 = 0.12$, from which the real process starts to be described by the hydrodynamic theory of impact.

Theory and experiment on the initial section of the curve of cavity collapse up to the beginning of oscillations are compared in Fig. 8 for $\varepsilon = 0.025$, $\lambda = 7.8 \cdot 10^{-2}$, and $\delta = 8.7 \cdot 10^{-2}$, with curve 1 for $\beta = 0.25$ and curve 2 for $\beta = 0.0625$.

Test data for $\beta = 0.25$, $\delta = 4.0 \pm 1.5$, and different values of the parameter λ which characterizes the inertial force, $\lambda = 0.312$ (point 1), $\lambda = 0.555$ (point 2), and $\lambda = 1.25$ (point 3) are presented in Fig. 9 (upper part of the graph). The experimental results lie well along one curve. This is indeed natural since the counterpressure sharply hinders motion of the cavity boundary only in the concluding stage of collapse.

Presented in the same Fig. 9 (lower part of the graph) are test data for $\beta = 0.25$, $\lambda = 0.43 \pm 0.12$, and different values of the parameter ν characterizing the influence of viscosity. The different slope of the two groups of tests can be explained by the predominating influence of the inertial forces on the lower curve (the points 5), where the parameter $\nu \approx 0.1$ in (25) is still sufficiently small as compared with the other coefficients. As the influence of the viscosity rises, the slope of the collapse curves diminishes (the group of points 5 where $\nu \approx 1$).

Also noticed in the tests was the dependence of the beginning of the origination of instability on the magnitude of the Reynolds number R_*. This fact can be explained by the perturbing influence of the growing boundary layer on the inertial velocity profile.

Pictured in Fig. 10 is the experimental dependence of the Reynolds number $R_* = \rho_0 U_* h_* / \mu$ at the time of the origination of instability (the formation of a cumulative jet on the cavity boundary) as a function of the parameter

$$\varkappa = 1/\varepsilon_* \sqrt{R} \sim \delta_* / h_{*i} \qquad R = \rho_0 a u_* / \mu$$

where δ_* is the boundary-layer thickness.

The character of the collapse of a cylindrical cavity for $\beta = 0.0625$, $\varepsilon = 0.05$, and the impact velocity $w_0 = 2$ m/sec can be observed in Fig. 11, where a series of frames from an exposure by a ZhLV-2 time magnifier is presented (the numbers under the frames denote the time in microseconds from the beginning of the motion of the cavity boundary).

Let us note the origin of instability (a cumulative jet) and the presence of cavitation bubbles in the fluid, which possibly originate in the first instants of impact because of tension of the fluid during interaction of the side unloading waves. The character of the flow near the neutral line opposite to the pressure gradient is also influential in this same direction.

The authors are grateful to A. M. Kogan and L. V. Mostovaya for performing the computations.

LITERATURE CITED

1. Lord Rayleigh, "On the pressure developed in a liquid during collapse of a spherical cavity," Phil. Mag., 34, 94 (1917).
2. E. I. Zababakhin, "Filling of bubbles in a viscous fluid," Prikl. Mat. i Mekhan., 24, No. 6 (1960).
3. C. Hunter, "On the collapse of an empty cavity in water," J. Fluid Mech., 8, 2 (1960).
4. A. Yu. Ishlinskii, "On the plane motion of sand," Ukr. Mat. Zh., 6, No. 4 (1954).
5. M. A. Lavrent'ev, "Cumulative charge and principles of its operation," Usp. Matem. Nauk, 12, No. 4 (1957).
6. Yu. B. Khariton, "On the question of detonation from impact," in: Papers on the Theory of Explosives [in Russian], Oborongiz, Moscow (1940), pp. 177-196.
7. F. P. Bowden and A. D. Jaffe, Excitation and Development of an Explosion in Solid and Liquid Materials [Russian translation], IL, Moscow (1955).
8. G. I. Pokrovskii, Explosions [in Russian], Nedra, Moscow (1964).
9. É. I. Andriankin, "Spreading of a viscous drop under impact," Prikl. Mekhan. i Tekhn. Fiz., No. 5 (1966).
10. V. K. Bobolev and A. V. Dubovik, "Cumulative jets in the collapse of cavities in thin fluid layers," Prikl. Mekhan. i Tekh. Fiz., No. 2 (1970).